ACS APPLIED MATERIALS & INTERFACES

RESEARCH ARTICLE

www.acsami.org

Colorimetric Assay of Lead Ions in Biological Samples Using a Nanogold-Based Membrane

Yen-Fei Lee[†,‡] and Chih-Ching Huang*[,†,‡]

[†]Institute of Bioscience and Biotechnology and [‡]Center of Excellence for Marine Bioenvironment and Biotechnology (CMBB), National Taiwan Ocean University, 2, Beining Road, Keelung 20224, Taiwan

Supporting Information

ABSTRACT: We have developed a simple paper-based colorimetric membrane for sensing lead ions (Pb^{2+}) in aqueous solutions. The nitrocellulose membrane (NCM) was used to trap bovine serum albumin (BSA) modified 13.3-nm Au nanoparticles (BSA-Au NPs), leading to the preparation of a nanocomposite film of a BSA-Au NP-decorated membrane (BSA-Au NPs/NCM). The BSA-Au NPs/NCM operates on the principle that Pb^{2+} ions accelerate the rate of leaching of Au NPs induced by thiosulfate ($S_2O_3^{2-}$) and 2-mercaptoethanol (2-ME). The BSA-Au NPs/NCM allowed for the detection of Pb^{2+} by the naked eye in nanomolar aqueous solutions in the presence of leaching agents such as $S_2O_3^{2-}$ and 2-ME. We employed the assistance of microwave irradiation to shorten the reaction time (<10 min) for leaching the Au NPs. Under optimal solution conditions (5 mM glycine−NaOH (pH 10), $S_2O_3^{2-}$ (100 mM), and 2-ME (250 mM), microwaves (450 W)), the BSA-Au NPs/NCM allowed the detection of Pb^{2+} at concentrations as low as 50 pM with high selectivity (at least 100-fold over other metal ions). This cost-effective sensing system allowed for the rapid and simple determination of the concentrations of Pb^{2+} ions in real samples (in this case, sea water, urine, and blood samples).

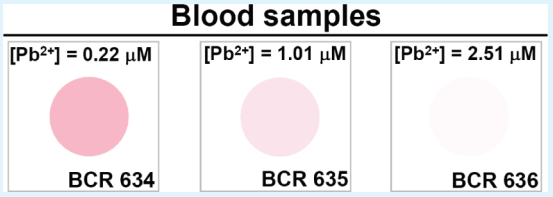

KEYWORDS: gold nanoparticles, membrane, colorimetric assay, lead ions, blood

1. INTRODUCTION

Lead (Pb) is well-known for its toxicity and wide distribution in the global environment.[1−4] Currently, the largest industrial use of lead is in the production of lead batteries, which are extensively used in the automobile industry.[5,6] All forms of Pb are toxic and adversely affect reproductive, nervous, immune, and cardiovascular systems as well as developmental processes in children.[7−10] Once Pb is introduced into the body, it becomes a potent neurotoxin that can interfere with brain development, slow nerve conduction velocity, and trigger behavioral problems.[11−14] The action level for lead in drinking water is defined by the U.S. Environmental Protection Agency (EPA) as 15 ppb.[15] The World Health Organization (WHO) has defined the whole blood lead concentrations >300 ppb in adults as indicative of significant exposure and recommends chelation therapy when the whole blood lead concentration exceeds 600 ppb.[16,17] The Agency for Toxic Substances and Disease Registry of the United States has defined the action level for lead in urine as 23 ppb.[18] The biomonitoring of Pb in urine and blood enables the quantitative evaluation of human exposure to both occupational and environmental Pb hazards. Concentrations of Pb in urine and blood have been used as indicators of exposure to lead.[19,20]

Concerns over toxic exposure to Pb have motivated the exploration of new methods for monitoring the concentrations of aqueous Pb^{2+} ions in environmental and biological samples. Several traditional quantitative methods for Pb^{2+} detection have been developed in the past decade, using such techniques as flame atomic absorption spectrometry, graphite furnace atomic absorption spectrometry, anode stripping voltammetry, inductively coupled plasma-atomic emission spectroscopy, inductively coupled plasma mass spectrometry (ICP-MS), X-ray fluorescence spectroscopy, neutron activation analysis, differential pulse anode stripping voltammetry, and isotope dilution mass spectrometry.[21−26] Although these methods can be used to detect Pb on the parts per billion scale, the instruments required are expensive and cumbersome to operate.

The past few years have witnessed great progress in the development of optical techniques for the detection of Pb^{2+} ions using small molecules,[27−33] DNAzymes,[34−42] oligonucleotides,[43,44] polymers,[45−47] proteins,[48,49] and nanomaterials[50−65] which have been demonstrated to be useful for the selective detection of Pb^{2+} ions in aqueous solutions. Nevertheless, many of these systems have limiting conditions such as poor aqueous solubility, cross-sensitivity toward other metal ions, matrix interference, high cost, complicated processing, the use of unstable molecules, or poor sensitivity. In addition these techniques are few applied to determination of Pb^{2+} in real biological samples. Previously, we developed a colorimetric, nonaggregation-based gold nanoparticle (Au NP) probe for the detection of Pb^{2+} ions in aqueous solutions, based on the fact that Pb^{2+} ions accelerate the rate of leaching of Au NPs induced by thiosulfate ($S_2O_3^{2-}$) and 2-mercaptoethanol (2-ME).[66] Monitoring the surface plasmon

Received: May 1, 2011
Accepted: June 23, 2011
Published: June 23, 2011

dx.doi.org/10.1021/am200535s | ACS Appl. Mater. Interfaces 2011, 3, 2747–2754

resonance (SPR) of the Au NPs allowed us to quantify the level of Pb^{2+} ions in the solution. Although this nanosensor allowed for highly selective sensing of Pb^{2+} ions in the nanomolar range, it did not function in high-salinity solutions, exhibiting the same limitation observed for other Au-NP-based label-free assays.[66−74] Moreover, its analysis time was greater than 2 h. Therefore, we developed a simple paper-based colorimetric sensor for rapidly detecting Pb^{2+} ions with a Au NP modified nitrocellulose membrane (NCM) in this study. The NCM (0.5 cm × 0.5 cm) was used to trap bovine serum albumin (BSA) modified 13.3-nm Au NPs (BSA-Au NPs) through superior hydrophobic interactions between the NCM and BSA,[75−77] leading to a nanocomposite film of BSA-Au NPs on the membrane (BSA-Au NPs/NCM). The BSA-Au NPs/NCM allowed for the detection of Pb^{2+} in the nanomolar range in aqueous solutions in the presence of $Na_2S_2O_3$ and 2-ME by the naked eye. We carefully evaluated the roles played by the concentrations of $S_2O_3^{2-}$ and 2-ME in determining the sensitivity and selectivity of this probe for Pb^{2+}. Furthermore, to speed up the analysis time and improve the sensitivity, we used a BSA-Au NPs/NCM under microwave irradiation to sense Pb^{2+} ions. We also demonstrated the practicality of using this approach for the determination of Pb^{2+} ions in highly concentrated saline seawater and as well as complicated biological urine and blood samples.

2. EXPERIMENTAL DETAILS

2.1. Chemicals. 2-Mercaptoethanol (2-ME), sodium thiosulfate ($Na_2S_2O_3$), trisodium citrate, bovine serum albumin (BSA), glycine, and all the metal salts used in this study were purchased from Sigma-Aldrich (Milwaukee, WI). Tetrachloroauric(III) acid ($HAuCl_4$) was purchased from Acros (Geel, Belgium). The water used in all experiments was ultrapure water from a Milli-Q system. The buffer (glycine-NaOH) comprised of 50 mM glycine (pH 10) adjusted with 1.0 N NaOH. The purities of all chemicals were greater than 95% and were used without further purification. Urine samples (SRM 2672a) were obtained from the National Institute of Standards and Technology (NIST; Gaithersburg, MD). The NCM was purchased from GE Healthcare Bioscience, New Jersey. BCR 636, 635, and 634 human blood samples was purchased from IRMM (Institute for Reference Materials and Measurement; Geel, Belgium).

2.2. 13.3-nm Spherical Au NPs. The 13.3-nm-diameter spherical Au NPs were prepared through citrate-mediated reduction of $HAuCl_4$.[78−81] Aqueous 1 mM $HAuCl_4$ (250 mL) was brought to a vigorous boil by stirring in a round-bottom flask fitted with a reflux condenser; 38.8 mM trisodium citrate (25 mL) was added rapidly to the solution, and the solution was heated for another 15 min, turning from pale yellow to deep red. The solution was cooled to room temperature by stirring continuously. The sizes of the Au NPs were verified using transmission electron microscopy (TEM, H7100, Hitachi High-Technologies Corporation; Tokyo, Japan). They appeared to be nearly monodisperse with an average size of 13.3 ± 0.6 nm. A μ-Quant microplate reader (Biotek Instruments, Winooski, VT) was used to measure the absorbance of the Au NP solution. The particle concentration of the Au NPs (15 nM) was determined according to Beer's law using an extinction coefficient of $2.08 \times 10^8\ M^{-1}\ cm^{-1}$ at 520 nm for the 13.3-nm Au NPs.

2.3. Fabrication of the BSA-Au NPs/NCM. To prepare the BSA-modified Au NPs (BSA-Au NPs), an aliquot of the BSA solution (3 μM, 20 mL) was added to the 13-nm Au NP solution (15 nM, 20 mL) and equilibrated for 30 min at 25 °C. From flocculation assays, we estimated the average number of BSA molecules on a Au NP to be ∼20. A piece of NCM was cut to a size 0.5 cm (length) × 0.5 cm (width) and dipped with the BSA-Au NPs solution (15 nM, 1 μL). After drying in air for 15 min, the BSA-Au NP-modified NCM (BSA-Au NPs/NCM) was gently washed with DI water (∼20 mL) for 30 s to remove any weakly bonded BSA-Au NPs or impurities and then dried in air at room temperature for 1 h prior to use. The BSA-Au NPs/NCM probes were stable for at least 6 months when stored at 4 °C in the dark. The image of the BSA-Au NPs/NCM for color analysis was obtained using an Epson desktop scanner (Epson Perfection 1660 Photo Scanner). Color analysis was performed using an Image J computer program that measured the red, green, and blue (RGB) color intensities (each 8-bit channel with brightness values from 0 to 255) for pixels within the scanner image. The green component (intensity from 0 to 255) of the image of the BSA-Au NP/NCM was used to quantify the Au NPs.

2.4. Detecting Pb^{2+} Ions with the BSA-Au NPs/NCM. To sense Pb^{2+} ions, the as-prepared BSA-Au NPs/NCM was immersed in an aliquot (1 mL) of 5 mM glycine−NaOH (pH 10) solution, containing $Na_2S_2O_3$ (100 mM), 2-ME (250 mM), and Pb^{2+} ions (0−10 μM) and, then, equilibrated at room temperature for 2 h. Furthermore, the membrane was gently washed with DI water (∼5 mL) for 30 s and dried with an air blow gun (60 lb/in^2) for 1 min prior to analysis.

2.5. Surface-Assisted Laser Desorption/Ionization Mass Spectrometry of the BSA-Au NPs/NCM. The BSA-Au NPs/NCM was attached to a matrix-assisted laser desorption/inoization (MALDI) plate with adhesive polyimide film tape prior to the surface-assisted laser desorption/ionization mass spectrometry (SALDI-MS) measurements. Mass spectrometry experiments were performed in the reflectron positive-ion mode using an AutoflexIII MALDI-TOF/TOF mass spectrometer (Bruker Daltonics; Bremen, Germany). The samples were irradiated with a nitrogen laser (output at 337 nm) at 10 Hz. Ions produced by laser desorption were stabilized energetically during a delayed extraction period of 200 ns and then accelerated through the time-of-flight (TOF) chamber in the reflection mode prior to entering the mass analyzer. The available accelerating voltages ranged from +20 to −20 kV. The instruments were calibrated using Au clusters ($[Au_x]^+$, $x = 1-3$). A total of 1000 pulsed laser shots were applied, and we accumulated those signals from 10 MALDI target positions under a laser fluence of 75 μJ.

2.6. Analysis of Seawater, Urine, and Blood Samples. A sample of seawater from the East China Sea was filtered through a 0.2-μm membrane and analyzed using an ICP-MS. Aliquots of the seawater (0.5 mL) were spiked with standard Pb^{2+} solutions (100 μL) of final concentrations in the range 0−10 nM. The mixtures were diluted to 1.0 mL with 5 mM glycine−NaOH (pH 10) containing $Na_2S_2O_3$ (100 mM) and 2-ME (250 mM) and, then, analyzed using the present approach with the BSA-Au NPs/NCM probe under irradiation of microwave (450 W).

The preparation of the sample for the detection of Pb^{2+} ions in urine (SRM 2672a) was performed according to the standard method (1180B/05-OD) published by the National Center for Environmental Health.[82] The certified concentration of Pb^{2+} ions in this urine sample was 1.20 μM. Aliquots of the 200-fold-diluted urine samples (250 μL) were spiked with standard Pb^{2+} solutions of final concentrations in the range 0−1.0 nM. The spiked samples were then diluted to 500 μL with 5 mM glycine−NaOH (pH 10), containing $Na_2S_2O_3$ (100 mM) and 2-ME (250 mM), and then analyzed using the present approach

Scheme 1. Schematic Representation of the Preparation of BSA-Au NPs/NCM for Sensing Lead Ions (Pb^{2+}) Based on Accelerated the Leaching Rate of BSA-Au NPs by Sodium Thiosulfate and 2-Mercaptiethanol

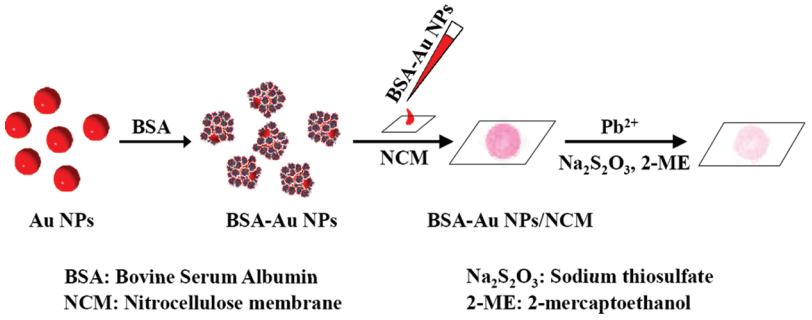

with the BSA-Au NPs/NCM probe under irradiation of microwave (450 W).

BCR 636, 635, and 634 human bloods was analyzed as a lyophilized material (0.6 g) and was reconstituted with 3 mL of DI water to obtain a 2.51 ± 0.24, 1.01 ± 0.12, and 0.22 ± 0.02 μM Pb blood reference sample, respectively.[83] The blood sample preparation generally followed the procedure reported earlier.[84] Briefly, 1 mL of blood was diluted with 8 mL of DI water and then treated with 1 mL of concentrated HNO_3 for 2 h. The sample was briefly centrifuged at 4000 rpm for 2 min. The supernatant was diluted with DI water and then analyzed using the present approach with the BSA-Au NPs/NCM probe under irradiation of microwave (450 W).

3. RESULTS AND DISCUSSION

3.1. Preparation of the BSA-Au NPs/NCM. Scheme 1 depicts the preparation protocol for the fabrication of the BSA-Au NPs/NCM substrate that was used for the detection of Pb^{2+} ions. Because the surfaces of the Au NPs were capped with citrate, which contains anionic carboxylate groups at pH > 3.0, the NPs attract the positively charged regions of the BSA surfaces through electrostatic attraction to form BSA-modified Au NPs (BSA-Au NPs).[85] From dynamic light scattering (DLS) measurements, we estimated the hydrodynamic diameters of the unlabeled Au NPs and BSA-Au NP assemblies to be 28.3 ($\pm$ 6.2) and 45.2 ($\pm$ 7.5) nm, respectively. The as-prepared BSA-Au NPs retained their stability in solutions containing up to 500 mM NaCl. In addition, the BSA-Au NPs could be stored in lyophilized solid form. The steric repulsive force between the BSA-Au NPs was the main contributor towards the dispersion of BSA-Au NPs in the solution, a contribution from electrostatic repulsion was also probably involved. The NCM has been widely used as a blotting matrix for protein immobilizations.[86] In these cases, hydrophobic interactions between proteins and nitrocellulose are mainly responsible for the adsorption of proteins onto the membrane, while impurities such as small molecules and ions could be removed by washing. We characterized of the as-prepared BSA-Au NPs/NCM by scanning electron microscopy (SEM), energy-dispersive X-ray spectroscopy (EDS), and reflection-mode UV-vis absorbance spectrometry. The SEM and high magnified SEM images of the BSA-Au NPs/NCM confirmed that the Au NPs adsorbed on the NCM surfaces did not form aggregates (Supporting Information Figure S1A and S1D). The EDS measurements were conducted to confirm the presence of the Au NPs at the surface of the BSA-Au NPs/NCM (Supporting Information Figure S2). No obvious differences appeared in the surface plasmon resonance (SPR) absorption bands at 520 nm of the citrate-capped Au NPs solution, BSA-Au NPs solution, BSA-Au NP/NCM, suggesting that most of the BSA-Au NPs were dispersed without aggregation on the NCM (Supporting Information Figure S3). This data was consistent with the photographic images of the BSA-Au NPs/NCM (see the top photographic images of Figure 1B) that clearly display the deposition of Au NPs (rose red) on the NCM (white membrane) to form the BSA-Au NPs/NCM (homogenous pink). Analysis of the color and surface-assisted laser desorption/ionization mass spectrometry (SALDI-MS) images of the BSA-Au NPs/NCM shown in Supporting Information Figure S4 further confirmed that the NC fibers associated homogenously with the adsorbed BSA-Au NPs. The RSDs of profile analyses in color and SALDI-MS image were 1.8% and 4.1%, respectively. From the ICP-MS data, we estimated that there were 2.95×10^{-8} mg Au NPs per NCM (0.5 cm $\times$ 0.5 cm).

3.2. Sensing of Pb^{2+} Ions. When the BSA-Au NPs (1.5 nM) reacted with $S_2O_3^{2-}$ ions (1.0 mM) in a 5 mM glycine–NaOH (pH 10) solution, $S_2O_3^{2-}$ penetrated into the BSA layer and $Au(S_2O_3)_2^{3-}$ complexes were formed immediately on the Au NP surfaces. The addition of Pb^{2+} ions (1.0 μM) and 2-ME (100 mM) induced the deposition of Pb on the surfaces of the Au NPs. The deposition of Pb accelerated the dissolution of the Au NPs, forming Au^{+}-2-ME complexes in the solution.[66] As a result, the SPR absorbance of the BSA-Au NPs at 520 nm decreased dramatically (see Figure 1A).

Because of the observation that $S_2O_3^{2-}$ and 2-ME could accelerate the leaching of the BSA-Au NPs by the Pb^{2+} ions, we further tested the BSA-Au NPs/NCM composite for the sensing of Pb^{2+} ions. In a proof-of-concept experiment, we recorded the green component absorbance (G_{abs}) of the BSA-Au NPs/NCM after it reacted with the leaching agents (100 mM $Na_2S_2O_3$ and 250 mM 2-ME) in the absence and presence of Pb^{2+} (1.0 μM). G_{abs} (8-bit, with brightness values from 0 to 255) are related to the quantitation of Au NPs. A high value of G_{abs} indicates a decrease in the intensity of observed red color and thus high amount of leaching of Au NPs. Data point a in Figure 1B indicates BSA-Au NPs with intense and homogenous color. Data point c reveals that $PbCl_2$ (1.0 μM) accelerated the dissolution of the Au NPs on the NCM in the presence of 100 mM $S_2O_3^{2-}$ and 250 mM 2-ME, resulting in a large increase in G_{abs}. In addition, we took advantage of the high reproducibility of SALDI-MS and its simple sample preparation techniques to prove the formation of Pb–Au alloy on the Au NP surfaces during the acceleration of the leaching rate (see Supporting Information Figure S5).[66,87−89] As indicated in Supporting Information Figure S6, which displays

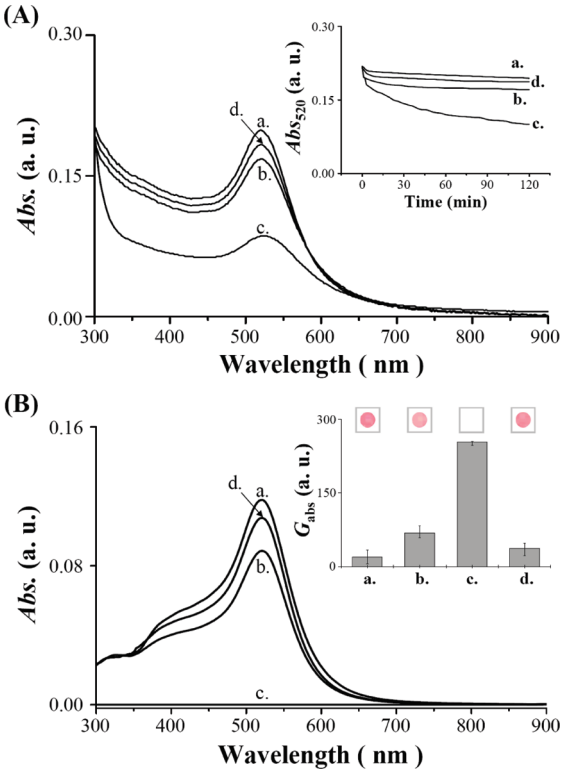

Figure 1. UV−vis absorption spectra of (A) the BSA-Au NP solutions and (B) the BSA-Au NP/NCM probes, recorded in transmission and reflection mode, respectively. (A, inset) Time-course measurements of values of UV-vis absorbance at 520 nm (Abs_{520}) of solutions containing (a) BSA-Au NPs (1.5 nM); (b) BSA-Au NPs (1.5 nM), $Na_2S_2O_3$ (1.0 mM), and 2-ME (100 mM); (c) BSA-Au NPs (1.5 nM), $Na_2S_2O_3$ (1.0 mM), 2-ME (100 mM), and $PbCl_2$ (1.0 μM); (d) BSA-Au NPs (1.5 nM) and $PbCl_2$ (1.0 μM). (B, inset) (top) Photographic images of the colors and (bottom) G_{abs} values of the BSA-Au NPs/NCM alone (a) and reacted with various mixtures (b) $Na_2S_2O_3$ (100 mM) and 2-ME (250 mM); (c) $Na_2S_2O_3$ (100 mM), 2-ME (250 mM), and $PbCl_2$ (1.0 μM); (d) $PbCl_2$ (1.0 μM). Buffer: 5 mM glycine−NaOH solution (pH 10). Mixtures were reacted for 2 h. Abs_{520} and G_{abs} are plotted in arbitrary units (a. u.). Error bars in part B are standard deviation values across four repetitive experiments.

a plot of G_{abs} of the BSA-Au NPs/NCM, Pb^{2+}-induced leaching of the BSA-Au NPs on the NCM reached completion within 2 h. In contrast, only a slight increase in the green component absorbance of the BSA-Au NPs/NCM occurred in the presence of $S_2O_3^{2-}$ and 2-ME (b in Figure 1B). Compared with our previous Au NP probe using $S_2O_3^{2-}$ (1.0 mM) and 2-ME (1.0 mM), the relatively high concentration of $S_2O_3^{2-}$ (100 mM) and 2-ME (250 mM) used in this study resulted in acceleration of the leaching of BSA-Au NPs/NCM. The SEM image of the BSA-Au NPs/NCM in Supporting Information Figure S1 reveals that the Pb^{2+} induced almost complete leaching of Au NPs by the leaching agents (100 mM $S_2O_3^{2-}$ and 250 mM 2-ME) in the presence of 1.0 μM $PbCl_2$.

3.3. Effects of 2-ME. The effect of pH on the leaching of 2-ME/$S_2O_3^{2-}$−Au NPs in the presence of Pb^{2+} have been studied in our previous report.[66] We found that Pb^{2+} ions accelerated the dissolution of the Au NPs, which reached a maximum value at pH 10. We further investigated the effects of 2-ME concentration (0−2.5 M) on the leaching of Au NPs in 5 mM glycine-NaOH (pH 10) in the absence and presence of Pb^{2+} ions (0.1 nM−10 μM). The rate of dissolution of BSA-Au NPs on the NCM in the 2-ME/$S_2O_3^{2-}$ solution increased on increasing the concentration of 2-ME in the absence of Pb^{2+} ions (Figure 2). In addition, the rate of leaching increased on increasing the concentration of Pb^{2+} ions (10 nM−1.0 μM) in the presence of a constant concentration of 2-ME (within the range 100 mM−2.5 M). Retardation of gold dissolution at concentrations of Pb^{2+} greater than 1.0 μM might be possible because of the formation of passive layers of PbS on the surface of Au NPs. Although the 2-ME (2.5 M)/$S_2O_3^{2-}$ (100 mM) solution provided the best sensitivity for the detection of Pb^{2+} ions, the reproducibility was poor (RSD = ~8.2%) and the linear range was narrow (10−100 nM). When using solutions of 2-ME (250 mM)/$S_2O_3^{2-}$ (100 mM), we obtained a linear relationship (R^2 = 0.98) between the values of G_{abs} of the Au NPs and the logarithm of the concentration of the Pb^{2+} ions in the range from 10 nM to 1.0 μM (see Figure 2). The limit of detection (LOD; signal/noise (S/N) ratio = 3) for the Pb^{2+} ions was 5 nM.

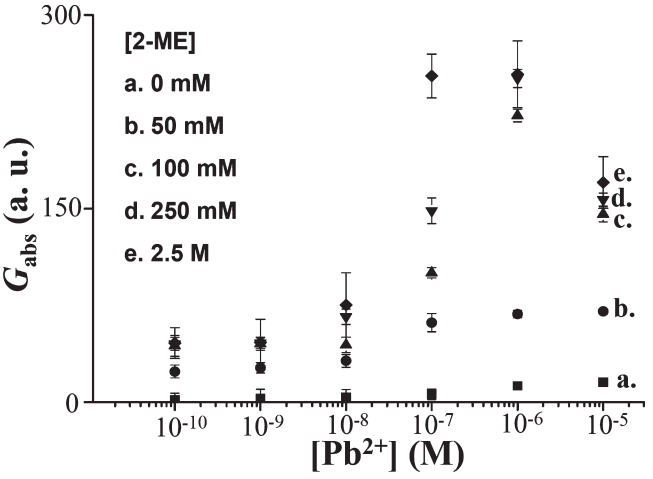

Figure 2. Effects of concentrations of 2-ME (0−2.5 M) on the values of G_{abs} of BSA-Au NPs/NCM in the presence of $PbCl_2$ (0.1 nM−10 μM) and leaching agents (100 mM $S_2O_3^{2-}$ and 0−2.5 M 2-ME). Other conditions were the same as those described in Figure 1.

3.4. Sensing Pb^{2+} under Microwave Irradiation. To shorten the analysis time (<10 min), we employed microwave irradiation to aid in leaching the Au NPs. Microwave-assisted leaching has been widely studied in an effort to improve the yields of extracted metal and to reduce process time.[90] Microwave (frequencies ~300 MHz−300 GHz) heating is one type of electroheating technique that utilizes specific wavelengths of electromagnetic energy.[91] When applying microwave irradiation to materials, the electric and magnetic components change rapidly, and the molecules cannot respond quickly to the change in direction, giving rise to friction and therefore causing them to warm up. The acceleration of the leaching rate of gold minerals under microwave irradiation was due to the superheating effect produced in a microwave field.[92−95] In addition, the different dielectric properties of the liquid and solid might result in localized temperature differences, creating strong convection currents at the surface of the microwaved solid.[96,97] Therefore, diffusions of the reaction products were rapidly promoted away from the surface. Figure 3A depicts the Pb^{2+} dose-dependent leaching of the BSA-Au NPs/NCM without and with microwave irradiation (400−500 W). The rate of dissolution of BSA-Au NPs on the NCM in the 2-ME/$S_2O_3^{2-}$ solution increased upon increasing the microwave power.

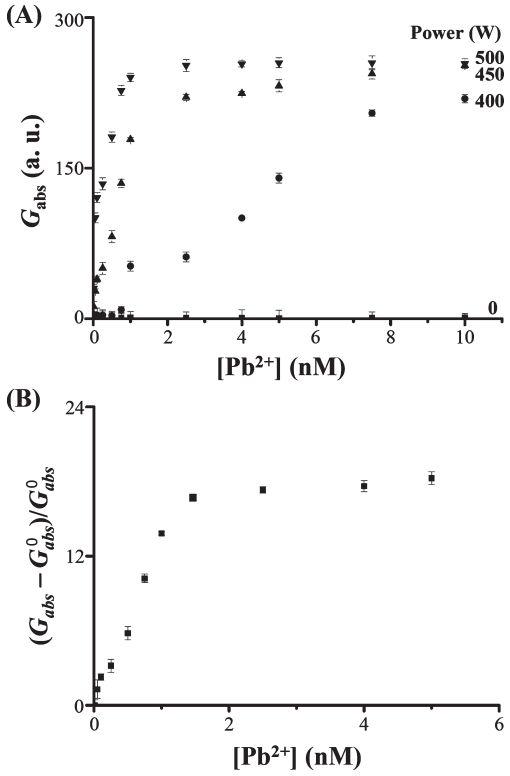

Figure 3. (A) Values of G_{abs} of the BSA-Au NPs/NCM probe in the presence of $PbCl_2$ (0−10 nM) and leaching agents (100 mM $S_2O_3^{2-}$ and 250 mM 2-ME) under microwave irradiation (0−500 W). (B) $[(G_{abs} - G^\circ_{abs})/G^\circ_{abs}]$ values of BSA-Au NPs/NCM probe in the presence of $PbCl_2$ (0−5 nM) and leaching agents (100 mM $S_2O_3^{2-}$ and 250 mM 2-ME) under microwave irradiation (450 W). Other conditions were the same as those described in Figure 1.

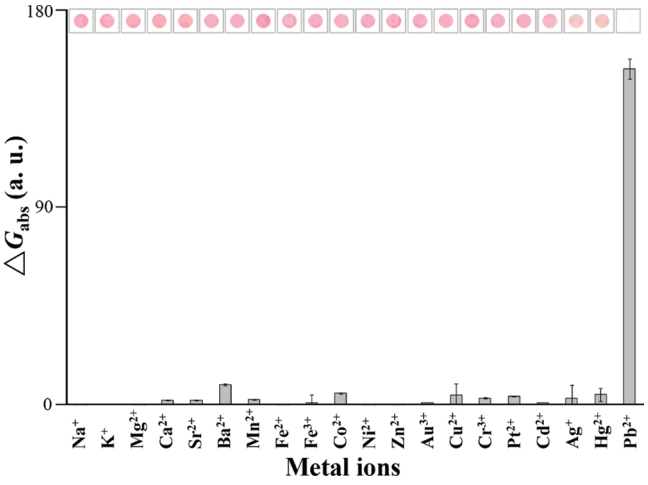

Figure 4. Selectivity of the BSA-Au NPs/NCM probe for Pb^{2+} ions. Concentration of Pb^{2+} ions was 10 nM; concentration of each of the other metal ions was 100 nM. Error bars represent standard deviations of four repeated experiments. Other conditions were the same as those described in Figure 3B.

In addition, the rate of leaching of gold increased upon increasing the concentration of Pb^{2+} ions (0−10 nM). We should note that the reaction times were shorter (10 min vs 2 h) under microwave irradiation (see Supporting Information Figure S7) than in the absence of microwave irradiation. At a constant concentration of 2-ME (250 mM) and $S_2O_3^{2-}$ (100 mM), we found that the optimal microwave power to sense Pb^{2+} was 450 W (see Figure 3B), based on the relationship between the signal enhancement ratio $[(G_{abs} - G^\circ_{abs})/G^\circ_{abs}]$ and the Pb^{2+} concentration. The descriptors G°_{abs} and G_{abs} represent the green component absorbance (G_{abs}) of the BSA-Au NPs/NCM probe in the absence and presence of Pb^{2+}, respectively. Under the optimal conditions (2-ME (250 mM), $S_2O_3^{2-}$ (100 mM), microwave (450 W)), we obtained a linear relationship ($R^2 = 0.96$) between the values of $[(G_{abs} - G^\circ_{abs})/G^\circ_{abs}]$ of the BSA-Au NPs/NCM and the concentration of Pb^{2+} ions in the range from 100 pM to 1.5 nM (see Figure 3B). The LOD (S/N ratio = 3) for the Pb^{2+} ions was ∼50 pM. One of the possible factors for this ultrahigh sensitivity for Pb^{2+} ions maybe the microwave temperature: under microwave irradiation of 400, 450, and 500 W, the reaction temperature was raised to ∼50, ∼75, and ∼90 °C, respectively (see Supporting Information Figure S8). The formation of passive layers of PbS on the surface of Au NPs was reduced under the higher temperatures, and thus retardation of the gold dissolution at concentrations of Pb^{2+} greater than 1.0 μM was not found. But we noted the reaction time was need 2 h to reach completion even at 90 °C condition (data not shown). This microwave-assisted leaching method not only shortened the analysis time to 10 min but also provided near two order of magnitude greater sensitivity than the above results.

3.5. Selectivity. Because our BSA-Au NPs/NCM allowed for the detection of Pb^{2+} at concentrations as low as 50 pM in the presence of 2-ME/$S_2O_3^{2-}$, we tested its selectivity by further investigating the changes in the values of G_{abs} of the BSA-Au NPs/NCM in the presence of 2-ME (250 mM)/$S_2O_3^{2-}$ (100 mM), one metal ion (Na^+, K^+, Mg^{2+}, Ca^{2+}, Sr^{2+}, Ba^{2+}, Mn^{2+}, Fe^{2+}, Fe^{3+}, Co^{2+}, Ni^{2+}, Zn^{2+}, Au^{3+}, Cu^{2+}, Cr^{3+}, Pt^{2+}, Cd^{2+}, Ag^+, or Hg^{2+} (100 nM)), and Pb^{2+} (10 nM) under microwave irradiation (450 W). As indicated in Figure 4, our paper-based probe responded selectively toward Pb^{2+} ions by a factor of 100 or more relative to the other metal ions. The tolerance concentrations of these metal ions for the sensing of Pb^{2+} using this approach were at least 10 times greater than the Pb^{2+} concentrations (data not shown). Because 2-ME and Hg^{2+} formed stable complexes in the bulk solution, formation of the Au−Hg amalgam did not occur.[66] The stronger affinities of alkanethiols {log $\beta[Hg(SR)_2]$ = ∼45, log $\beta[Ag(SR)_2]$ = ∼35} and $S_2O_3^{2-}$ {log $\beta[Hg(S_2O_3^{2-})_3^{4-}]$ = ∼31; log $\beta[Ag(S_2O_3^{2-})_2^{3-}]$ = ∼25} for Hg^{2+} and Ag^+ ions resulted in the formation of stable complexes in the bulk solution,[98,99] thereby inhibiting the formation of a Au−Hg amalgam or Ag−Au alloys on the surfaces of the $S_2O_3^{2-}$−Au NPs. Our reasoning was supported by the SALDI-MS and ICP-MS data; no Hg or Ag species were detected.

3.6. Detection of Lead Ions in Real Samples. We further tested the sensitivity of our BSA-Au NPs/NCM probe for Pb^{2+} ions in a solution containing salt that mimicked physiological conditions (150 mM NaCl, 5 mM KCl, 1 mM $MgCl_2$, 1 mM $CaCl_2$) (see Supporting Information Figure S9A), 250 μM cysteine (see Figure S9B), or 25 μM BSA (see Figure S9C), provided that the LOD values were approximately 100 pM. Our BSA-Au NPs/NCM showed a high tolerance to high concentrations of salts, aminothiols, proteins in real environmental or biological samples that might have induced the aggregation of particles, and the formation of complexes with the Pb^{2+} ions that interfere with the detection of the Pb^{2+}. Our results revealed the

Table 1. Determination of the Concentrations of Pb^{2+} in Urine (SRM 2672a) and Blood (BCR 634, 635, and 636) Samples by Microwave (450 W) Assisted $S_2O_3^{2-}$/2-ME-BSA-Au NPs/NCM Probe

sample	certified value (μM)	$S_2O_3^{2-}$/2-ME-BSA-Au NPs/NCM probe, mean ± SD (μM, n = 5)	spiked [Pb^{2+}] (nM)	R^2	consensus value (μM), 95% confidence interval[a]
SRM 2672a	1.20 ± 0.15	1.17 ± 0.071	0−1.00	0.97	1.08−1.26
BCR 634	0.22 ± 0.02	0.24 ± 0.013	0−0.75	0.94	0.22−0.26
BCR 635	1.01 ± 0.12	1.04 ± 0.150	0−0.50	0.98	0.85−1.23
BCR 636	2.51 ± 0.24	2.48 ± 0.212	0−0.50	0.98	2.22−2.74

[a] The t-test value is 2.77 at a 95% confidence level.

potential of this probe for the determination of the concentrations of Pb^{2+} ions in complicated, real samples.

To validate that our proposed sensing strategy could have practical applications for Pb^{2+} analysis in environmental samples, we used the BSA-Au NPs/NCM sensor to determine the levels of Pb^{2+} in a sea water sample. Here, we obtained linear correlations (R^2 = 0.96) between the values of $[(G_{abs} - G^{\circ}_{abs})/G^{\circ}_{abs}]$ and the concentration of the Pb^{2+} ions spiked in the two-fold diluted sea water in the range 100 pM−10 nM (see Supporting Information Figure S10) using the BSA-Au NPs/NCM probe in the presence of 2-ME (250 mM)/$S_2O_3^{2-}$ (100 mM). In these measurements, the BSA-Au NPs/NCM probe provided recoveries of 96%−105% of the Pb^{2+} ions. Neither our sensing approach nor the ICP-MS-based system detected the presence of Pb^{2+} ions in the original sea water sample.

We also utilized our sensor system to determine the Pb^{2+} concentrations in urine and blood samples because their levels can be indicative of exposure to lead. By applying standard addition methods to our new approach (see Supporting Information Figure S11A), we determined that the concentration of Pb^{2+} ions in the SRM 2672a urine sample (certified value: 1.20 μM) was 1.17 (± 0.071) μM (n = 5). Table 1 shows the results. Using a t-test (the t-test value was 2.776 with a 95% confidence level), the 95% confidence intervals for the Pb^{2+} ions were 1.08−1.26 μM, revealing that no significant differences existed between the values measured using our new approach and the certified values. Similarly, we determined that the concentration of Pb^{2+} ions in the BCR human blood samples by applying a standard addition method (see Supporting Information Figure S11B). Using a t-test, the 95% confidence intervals for the Pb^{2+} ions were in good agreement with the certified values (Table 1). In addition, the BSA-Au NPs/NCM probe could easily screen the Pb level in blood samples by naked eyes (Supporting Information Figure S12).

4. CONCLUSION

We have developed a simple, low-cost paper-based probe for the sensitive and selective colorimetric detection of Pb^{2+} ions using a BSA-Au NPs/NCM. The BSA-Au NPs/NCM allowed for the detection of Pb^{2+} in the subnanomolar range by the naked eye. The sensing of Pb^{2+}, assisted by microwave irradiation, shortened the analysis time to 10 min. This approach also demonstrated the high selectivity (by at least 100-fold over other metal ions) and sensitivity (LOD ~ 50 pM) for Pb^{2+} ions. The sensitivity of our assay to detect lead level in water is over two orders of magnitude higher than the EPA standard limit. In comparison with those nanoparticles- and oligonucleotides-based optical methods, our BSA-Au NPs/NCM probe for Pb^{2+} is relatively simple, cost-effective, selective, and sensitive.[34−44,50−65] Note that most other techniques require covalent conjugation of alkanethiol-ligands, thiolated-oligonucleotides to NPs or dye molecules to oligonucleotides. In addition, most of these probes tended to suffer from matrix interference, such as high concentrations of salts, aminothiols, and proteins, in real environmental or biological samples. This method should abrogate the need for synthesis of complicated chemosensors or the use of sophisticated equipment. Taking advantage of their high stabilities, the practicality of this method was validated with the analyses of seawater, urine, and blood samples. This simple, rapid, and cost-effective sensing system appears to hold great practical potential for the detection of heavy metal ions in real samples.

■ ASSOCIATED CONTENT

Supporting Information. Additional information as noted in the text. This information is available free of charge via the Internet at http://pubs.acs.org.

■ AUTHOR INFORMATION

Corresponding Author

*Tel./Fax: 011-886-2-2462-2034. E-mail: huanging@ntou.edu.tw.

■ ACKNOWLEDGMENT

This study was supported by the National Science Council of Taiwan under contract 99-2113-M-019-001-MY2.

■ REFERENCES

(1) Ahamed, M.; Siddiqui, M. K. J. *Clin. Nutr.* **2007**, *26*, 400–408.
(2) Gracia, R. C.; Snodgrass, W. R. *Am. J. Health-Syst. Pharm.* **2007**, *64*, 45–53.
(3) Murata, K.; Iwata, T.; Dakeishi, M.; Karita, K. *J. Occup. Health* **2009**, *51*, 1–12.
(4) Healey, N. *Radiat. Prot. Dosim.* **2009**, *134*, 143–151.
(5) Patil, A. J.; Bhagwat, V. R.; Patil, J. A.; Dongre, N. N.; Ambekar, J. G.; Jailkhani, R.; Das, K. K. *Int. J. Environ. Res. Public Health* **2006**, *3*, 329–337.
(6) Dartey, E.; Adimado, A. A.; Agyarko, K. *Environ. Monit. Assess* **2010**, *164*, 1–8.
(7) Basha, R.; Reddy, G. R. *Indian J. Exp. Biol.* **2010**, *48*, 636–641.
(8) Mishra, K. P. *Toxicol. Vitro* **2009**, *23*, 969–972.
(9) Poręba, R.; Gać, P.; Poręba, M.; Andrzejak, R. *Environ. Toxicol. Pharmacol.* **2011**, *31*, 267–277.
(10) Abelsohn, A. R.; Sanborn, M. *Can. Fam. Phys.* **2010**, *56*, 531–535.
(11) Ronco, A. M.; Gutierrez, Y.; Gras, N.; Muñoz, L.; Salazar, G.; Llanos, M. N. *Biol. Trace Elem. Res.* **2010**, *136*, 269–278.
(12) Olympio, K. P. K.; Gonçalves, C.; Günther, W. M. R.; Bechara, E. J. H. *Pan. Am. J. Public Health* **2009**, *26*, 266–275.
(13) Verstraeten, S. V.; Aimo, L.; Oteiza, P. I. *Arch. Toxicol.* **2008**, *82*, 789–802.

(14) Krieg, E. F., Jr; Chrislip, D. W.; Brightwell, W. S. *Arch. Toxicol.* **2008**, *82*, 531–542.
(15) http://water.epa.gov/drink/contaminants/basicinformation/lead.cfm (accessed April 2011).
(16) Fewtrell, L.; Kaufmann, R.; Prüss-Üstün, A. *Lead: Assessing the environmental burden of disease at national and local levels*; Environmental Burden of Disease Series; World Health Organization: Geneva, Switzerland, 2003; No. 2.
(17) WHO. *Exposure to lead: a major public health concern*; World Health Organization: Geneva, Switzerland, 2010.
(18) Agency for Toxic Substances and Disease Registry (ATSDR). *Toxicological profile for Lead*; U.S. Department of Health and Human Services, Public Health Service: Atlanta, GA, 2007.
(19) Rodrigues, E. G.; Virji, M. A.; McClean, M. D.; Weinberg, J.; Woskie, S.; Pepper, L. D. *J. Occup. Environ. Hyg.* **2010**, *7*, 80–87.
(20) Schütz, A.; Olsson, M.; Jensen, A.; Gerhardsson, L.; Börjesson, J.; Mattsson, S.; Skerfving, S. *Int. Arch. Occup. Environ. Health* **2005**, *78*, 35–43.
(21) Ghaedi, M.; Shokrollahi, A.; Niknam, K.; Niknam, E.; Najibi, A.; Soylak, M. *J. Hazard. Mater.* **2009**, *168*, 1022–1027.
(22) Bi, Z.; Chapman, C. S.; Salaün, P.; van den Berg, C. M. G. *Electroanalysis* **2010**, *22*, 2897–2907.
(23) Afonso, D. D.; Baytak, S.; Arslan, Z. *J. Anal. At. Spectrom.* **2010**, *25*, 726–729.
(24) Vantelon, D.; Lanzirotti, A.; Scheinost, A. C.; Kretzschmar, R. *Environ. Sci. Technol.* **2005**, *39*, 4808–4815.
(25) Inanez, J. G.; Speakman, R. J.; Garrigós, J. B. i.; Glascock, M. D. *Radiochim. Acta* **2010**, *98*, 525–531.
(26) Feng, L.; Wang, J.; Chao, J.; Lu, H. *J. Anal. At. Spectrom.* **2009**, *24*, 1676–1680.
(27) Meng, X.; Liu, L.; Guo, Q. *Prog. Chem.* **2005**, *17*, 45–54.
(28) Marbella, L.; Serli-Mitasev, B.; Basu, P. *Angew. Chem. Int. Ed.* **2009**, *48*, 3996–3998.
(29) Hu, Z. Q.; Lin, C. S.; Wang, X. M.; Ding, L.; Cui, C. L.; Liu, S. F.; Lu, H. Y. *Chem. Commun.* **2010**, 3765–3767.
(30) Goswami, S.; Chakrabarty, R. *Eur. J. Org. Chem.* **2010**, 3791–3795.
(31) Ju, H.; Lee, M. H.; Kim, J.; Kim, J. S.; Kim, J. *Talanta* **2011**, *83*, 1359–1363.
(32) Ma, L.; Li, H.; Wu, Y. *Sens. Actuators, B* **2009**, *143*, 25–29.
(33) Wang, J.; Chu, S.; Kong, F.; Luo, L.; Wang, Y.; Zou, Z. *Sens. Actuators, B* **2010**, *150*, 25–35.
(34) Li, C.-L.; Liu, K.-T.; Lin, Y.-W.; Chang, H.-T. *Anal. Chem.* **2011**, *83*, 225–230.
(35) Zhao, W.; Lam, J. C. F.; Chiuman, W.; Brook, M. A.; Li, Y. *Small* **2008**, *4*, 810–816.
(36) Lan, T.; Furuya, K.; Lu, Y. *Chem. Commun.* **2010**, 3896–3898.
(37) Yang, X.; Xu, J.; Tang, X.; Liu, H.; Tian, D. *Chem. Commun.* **2010**, 3107–3109.
(38) Zhang, L.; Han, B.; Li, T.; Wang, E. *Chem. Commun.* **2011**, 3099–3101.
(39) Xiang, Y.; Wang, Z.; Xing, H.; Wong, N. Y.; Lu, Y. *Anal. Chem.* **2010**, *82*, 4122–4129.
(40) Li, T.; Dong, S.; Wang, E. *J. Am. Chem. Soc.* **2010**, *132*, 13156–13157.
(41) Wang, F.; Wu, Z.; Lu, Y.; Wang, J.; Jiang, J. H.; Yu, R. Q. *Anal. Biochem.* **2010**, *405*, 168–173.
(42) Li, T.; Wang, E.; Dong, S. *Anal. Chem.* **2010**, *82*, 1515–1520.
(43) Liu, C.-W.; Huang, C.-C.; Chang, H.-T. *Anal. Chem.* **2009**, *81*, 2383–2387.
(44) Lin, Y.-W.; Liu, C.-W.; Chang, H.-T. *Talanta* **2011**, *84*, 324–329.
(45) Narkwiboonwong, P.; Tumcharern, G.; Potisatityuenyong, A.; Wacharasindhu, S.; Sukwattanasinitt, M. *Talanta* **2011**, *83*, 872–878.
(46) Luo, Q.; Guan, Y.; Zhang, Y.; Siddiq, M. *J. Polym. Sci., Part A: Polym. Chem.* **2010**, *48*, 4120–4127.
(47) Pramanik, S.; Sarkar, S.; Paul, H.; Chattopadhyay, P. *Indian J. Chem.* **2009**, *48A*, 30–37.
(48) Lin, T.-J.; Chung, M.-F. *Sensors* **2008**, *8*, 582–593.
(49) Shete, V. S.; Benson, D. E. *Biochemistry* **2009**, *48*, 462–470.
(50) Liu, D.; Wang, Z.; Jiang, X. *Nanoscale* **2011**, *3*, 1421–1433.
(51) Knecht, M. R.; Sethi, M. *Anal. Bioanal. Chem.* **2009**, *394*, 33–46.
(52) Lin, Y.-W.; Huang, C.-C.; Chang, H.-T. *Analyst* **2011**, *136*, 863–871.
(53) Ray, P. C.; Yu, H.; Fu, P. P. *J. Environ. Sci. Health., Part C Environ.* **2011**, *29*, 52–89.
(54) Zheng, Q.; Han, C.; Li, H. *Chem. Commun.* **2010**, 7337–7339.
(55) Son, H.; Lee, H. Y.; Lim, J. M.; Kang, D.; Han, W. S.; Lee, S. S.; Jung, S. H. *Chem.—Eur. J.* **2010**, *16*, 11549–11553.
(56) Beqa, L.; Singh, A. K.; Khan, S. A.; Senapati, D.; Arumugam, S. R.; Ray, P. C. *ACS Appl. Mater. Interfaces* **2011**, *3*, 668–673.
(57) Li, H.; Zheng, Q.; Han, C. *Analyst* **2010**, *135*, 1360–1364.
(58) Huang, K.-W.; Yu, C.-J.; Tseng, W.-L. *Biosens. Bioelectron.* **2010**, *25*, 984–989.
(59) Chai, F.; Wang, C.; Wang, T.; Li, L.; Su, Z. *ACS Appl. Mater. Interfaces* **2010**, *2*, 1466–1470.
(60) Alizadeh, A.; Khodaei, M. M.; Karami, C.; Workentin, M. S.; Shamsipur, M.; Sadeghi, M. *Nanotechnology* **2010**, *21*, 315503.
(61) Slocik, J. M.; Zabinski, J. S.; Phillips, D. M.; Naik, R. R. *Small* **2008**, *4*, 548–551.
(62) Kim, J. H.; Han, S. H.; Chung, B. H. *Biosens. Bioelectron.* **2011**, *26*, 2125–2129.
(63) Wang, X.; Guo, X. *Analyst* **2009**, *134*, 1348–1354.
(64) Wu, C.-S.; Oo, M. K. K.; Fan, X. *ACS Nano* **2010**, *4*, 5897–5904.
(65) Shen, L.; Chen, Z.; Li, Y.; He, S.; Xie, S.; Xu, X.; Liang, Z.; Meng, X.; Li, Q.; Zhu, Z.; Li, M.; Le, X. C.; Shao, Y. *Anal. Chem.* **2008**, *80*, 6323–6328.
(66) Chen, Y.-Y.; Chang, H.-T.; Shiang, Y.-C.; Hung, Y.-L.; Chiang, C.-K.; Huang, C.-C. *Anal. Chem.* **2009**, *81*, 9433–9439.
(67) Nath, N.; Chilkoti, A. *J. Fluoresc.* **2004**, *14*, 377–389.
(68) González, M. G.; Liu, X.; Niessner, R.; Haisch, C. *Sens. Actuators, B* **2010**, *150*, 770–773.
(69) Wei, H.; Li, B.; Li, J.; Dong, S.; Wang, E. *Nanotechnology* **2008**, *19*, 095501.
(70) Wang, Z.; Lee, J. H.; Lu, Y. *Adv. Mater.* **2008**, *20*, 3263–3267.
(71) Li, D.; Wieckowska, A.; Willner, I. *Angew. Chem. Int. Ed.* **2008**, *47*, 3927–3931.
(72) Liu, C.-W.; Hsieh, Y.-T.; Huang, C.-C.; Lin, Z.-H.; Chang, H.-T. *Chem. Commun.* **2008**, 2242–2244.
(73) Wang, Y.; Yang, F.; Yang, X. *Nanotechnology* **2010**, *21*, 205502.
(74) Wang, H.; Wang, Y.; Jin, J.; Yang, R. *Anal. Chem.* **2008**, *80*, 9021–9028.
(75) Helwa, R.; Hoheisel, J. D. *Anal. Bioanal. Chem.* **2010**, *398*, 2551–2561.
(76) Liu, J.; Liu, X.; Baeyens, W. R. G.; Delanghe, J. R.; Ouyang, J. *J. Proteome Res.* **2008**, *7*, 1884–1890.
(77) Burnette, W. N. *Anal. Biochem.* **1981**, *112*, 195–203.
(78) Turkevich, J.; Stevenson, P. C.; Hillier, J. *Discuss. Faraday Soc.* **1951**, *11*, 55–75.
(79) Enüstün, B. V.; Turkevich, J. *J. Am. Chem. Soc.* **1963**, *85*, 3317–3328.
(80) Turkevich, J. *Gold Bull.* **1985**, *18*, 86–91.
(81) Frens, G. *Nat Phys. Sci.* **1973**, *241*, 20–22.
(82) Jones, R. L. *Division of Laboratory Sciences Laboratory Protocol (Urinary Mercury, 1180B/05-OD)*; Centers for Disease Control and Prevention: Atlanta, GA, 2001.
(83) Byrialsen, K.; Kristiansen, J.; Christensen, J. M.; Discherl, C.; Gawlik, B. M.; Klein, C. L.; Lamberty, A. *The certification of the mass concentrations of lead and cadmium in reconstituted human blood*; European Commission, DG Joint Research Centre, Institute for Reference Materials and Measurements: Geel, Belgium, 2004.
(84) Brillas, E.; Mur, E.; Sauleda, R.; Sànchez, L.; Peral, J.; Domènech, X.; Casado, J. *Appl. Catal. B-Environ.* **1998**, *16*, 31–42.
(85) Brewer, S. H.; Glomm, W. R.; Johnson, M. C.; Knag, M. K.; Franzen, S. *Langmuir* **2005**, *21*, 9303–9307.
(86) Towbin, H.; Staehelin, T.; Gordon, J. *Proc. Natl. Acad. Sci. U. S. A.* **1979**, *76*, 4350–4354.
(87) Hung, Y.-L.; Hsiung, T.-M.; Chen, Y.-Y.; Huang, C.-C. *Talanta* **2010**, *82*, 516–522.

(88) Hung, Y.-L.; Hsiung, T.-M.; Chen, Y.-Y.; Huang, Y.-F.; Huang, C.-C. *J. Phys. Chem. C* **2010**, *114*, 16329–16334.
(89) Arakawa, R.; Kawasaki, H. *Anal. Sci.* **2010**, *26*, 1229–1240.
(90) Al-Harahsheh, M.; Kingman, S. W. *Hydrometallurgy* **2004**, *73*, 189–203.
(91) Kingston, H. M.; Haswell, S. J. *Microwave-enhanced chemistry: Fundamentals, sample preparation, and applications*; American Chemical Society: Washington, DC, 1997.
(92) Baghurst, D. R.; Mingos, D. M. P. *J. Chem. Soc., Chem. Commun.* **1992**, 674–677.
(93) Huang, J. H.; Rowson, N. A. *Hydrometallurgy* **2002**, *64*, 169–179.
(94) Elsamak, G. G.; Özta, N. A.; Yürüm, Y. *Fuel* **2003**, *82*, 531–537.
(95) Xia, D. K.; Picklesi, C. A. *Miner. Eng.* **2000**, *13*, 79–94.
(96) Nadkarni, R. A. *Anal. Chem.* **1984**, *56*, 2233–2237.
(97) Weian, D. *Rare Metals* **1997**, *16*, 153–155.
(98) Sillen, L. G.; Martell, A. E. In *Stability Constants of Metal-Ion Complexes: Supplement*; The Chemical Society: London, 1971.
(99) Morel, F. M. M.; Hering, J. G. In *Principles and Applications of Aquatic Chemistry*; Wiley: New York, 1993.